

STUDY OF PHYSICAL PROPERTIES OF SILVER NANOPARTICLES

Kulbir Singh

M.Sc. Physics, Lovely Professional University, Phagwara (PUNJAB).

ABSTRACT:

In the present investigation of silver (Ag) nanoparticles (NPs) of normal molecule size of 31-51 nm were set up by the warm disintegration technique within the sight of suitable centralization of Trioctylphosphine (TOP) and Oleylamine (OA). The X-beam diffraction estimations show the event of face-focused cubic metallic Ag-NPs. The compacted pellets of these nanoparticles were researched utilizing thermoelectric power in the temperature go from 5 to 300 K. The watched thermoelectric control for every one of the examples are ordinary of a decent metal and are seen as unequivocally reliant on grain size and the kind of capping utilized. The greatness of thermoelectric power increments as the molecule size diminishes. These outcomes obviously demonstrate predominant job of confusion at grain limits and quantum restriction, which impact dispersing of phonons and electrons in a noteworthy manner. UV-Visible spectroscopy uncovers the SPR retention band at 319 nm for Ag NPs tests arranged in ethylene glycol (EG). We accept that the red-move in SPR could be seen by utilizing diverse Surfactant/Capping agents.

Keywords: silver (Ag), nanoparticles (NPs), Oleylamine (OA), ethylene glycol (EG).

Experimental method

Silver nanoparticles were set up by warm disintegration strategy [Okram and kaurav 2011, Soni and Okram 2009]. At first 1.0 gram of silver acetic acid derivation was blended in with 5ml of Oleylamine (OA) and 100ml of ethylene glycol (EG) in a 100 ml 3-neck round jug flask, furnished with condenser and thermometer. The synthetic blend was warmed to 180°C. At the point when temperature arrived at 180°C, the refluxing courses of action were made. The shade of complex changed from grayish to light dark and afterward at long last almost dark after an interim of about 2hr which shows the commencement of arrangement of silver nanoparticles. The response was proceeded for an additional two hour. It was cooled to room temperature and

was isolated in the measuring utensil with the assistance of 20ml hexane and 50ml ethanol. At that point, the acquired hasten was washed with ultrasonic processor and 3-4 times by ethanol. Subsequent to washing the hasten the example was dried lastly it was acquired as dull dark powder. This example was coded as Ag-1. Essentially, subsequent to keeping every one of the parameters consistent, OA was taken 10ml and 15ml to plan second and third examples. They were coded as Ag-2 and Ag-3. Further Silver nanoparticles were set up by Trioctylphosphine instead of Oleylamine what's more, rest every single experimental condition were same.

This example was coded as Ag-4. So also, subsequent to keeping every one of the parameters consistent, TOP was taken 10ml and 20ml to get ready second and third examples. They were coded as Ag-5 and Ag-6. Further three examples of silver nanoparticles were likewise arranged by shifting mole proportion of Silver Acetate (CH_3COOAg) to EG ($\text{C}_2\text{H}_6\text{O}_2$) while fixing the convergence of EG at 100 ml. First example (Ag-7) was set up by 1 g of silver acetic acid derivation break up into 100 ml of EG. The arrangement was taken into three neck jar with refluxing game plan. The blends were warmed for four hours constantly between the temperature ranges 100 to 120°C . In the wake of cooling the blend up to room temperature, the accelerated material was taken out into another pot and blended 40 ml $\text{CH}_3)_2\text{CO}$ to wash the example.

The washing procedure was rehashed for 3 to multiple times and afterward test was dried. Staying two examples were readied with 0.50g (Ag-8) and 0.25g (Ag-9) silver acetic acid derivation focus while keeping the centralization of EG at 100 ml. The subtleties of generally speaking synthetic readiness of AgNPs are given in the Table 1. These NPs were examined by X-beam diffraction (XRD) utilizing Bruker D8 propelled X-beam diffractometer with $\text{Cu K}\alpha$ radiation in the 2θ territory from 30° to 90° . Thermopower estimation down to the fluid helium temperatures (5-300k) were done utilizing compacted pellet sandwiched between two oxygen free exceptionally leading squares and total thermopower was estimated with reference to Copper Square.

Results and discussion

XRD information of tests signified by Ag-1, Ag-2 and Ag-3 for different silver nanoparticles are appeared in Figure 1. Diffraction tops were watched and coordinated with standard JCPDS

information of two reports viz (87-0720), (75-0969) and cross section parameters were determined utilizing the coordinated (hkl) values. It is obvious from Figure 1 that all pinnacles relate to confront focused cubic structure of Ag-metal indicating that the examples arranged were of unadulterated silver metal nanoparticles.

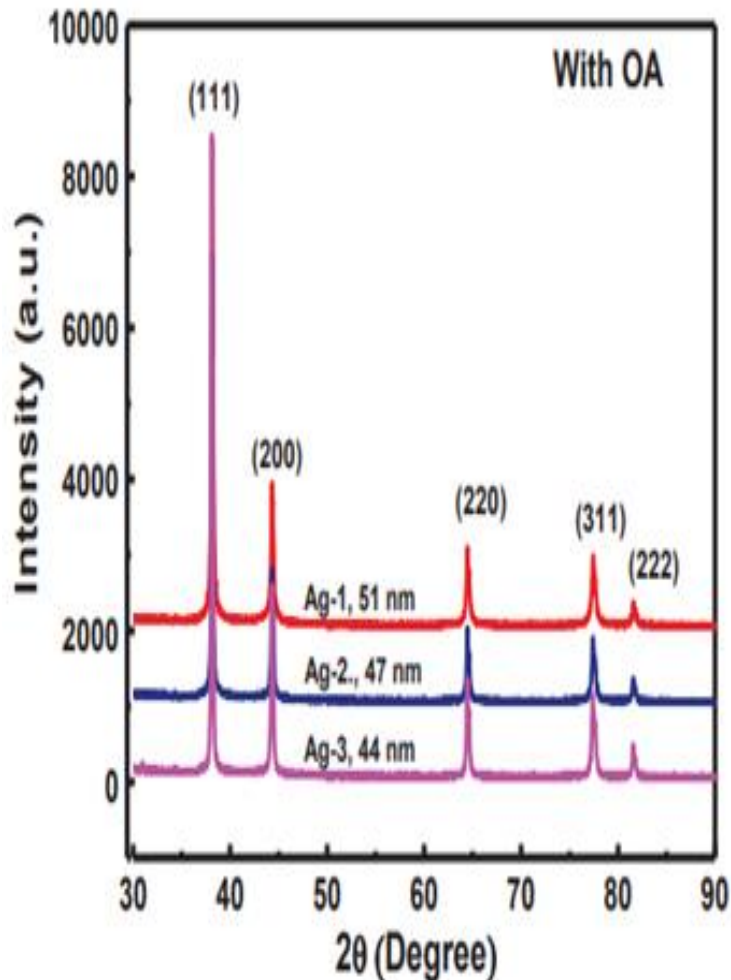


Figure 1. Shows the XRD patterns of AG-1,AG-2and AG-3 samples for Oleylamine content of 5ml, 10ml and 15 ml, respectively.

And XRD data of samples denoted by Ag-4, Ag-5 and Ag-6 for various silver nanoparticles prepared in various concentration of TOP are shown in Figure 2. Further the XRD data of silver nanoparticles samples were prepared by varying mole ratio of silver acetate (CH_3COOAg) is shown in Figure 3.

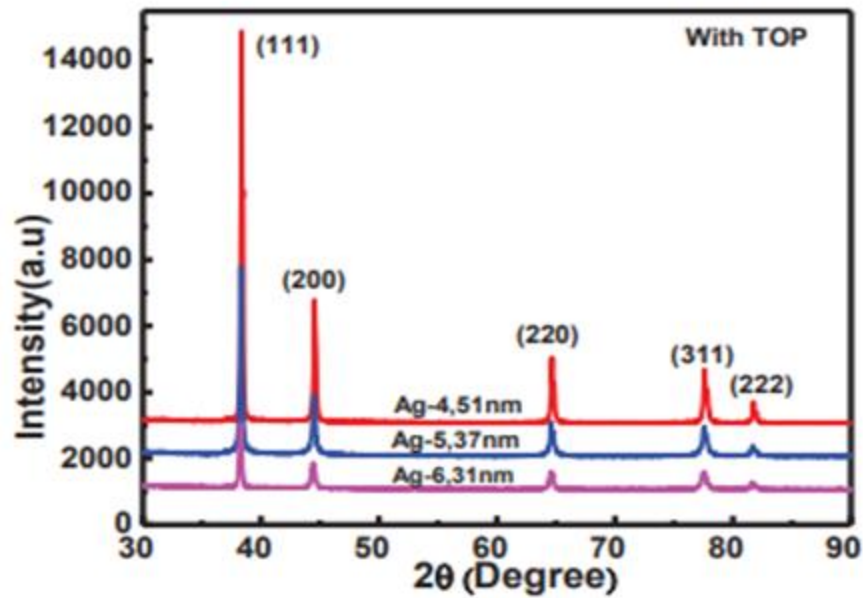


Figure 2. Shows the XRD patterns of AG-4, AG-5 and AG-6 samples for TOP content of 5ml, 10ml and 20 ml, respectively.

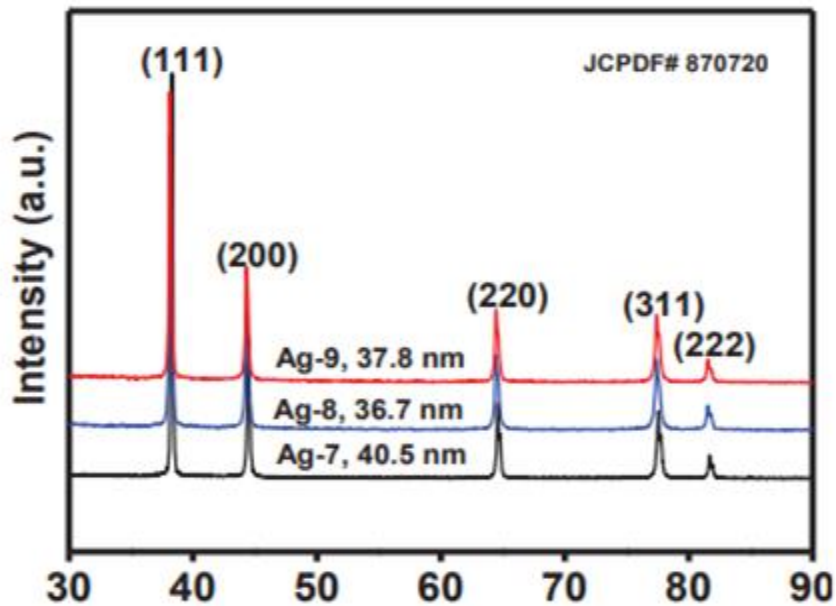


Figure 3. Shows the XRD patterns of AG-7, AG-8 and AG-9 samples for **Silver Acetate** content of 1 g, 0.50 g and 0.25 g, respectively.

The watched diffraction tops were coordinated with standard JCPDS information of two reports and cross section parameters were determined utilizing the coordinated (hkl) values. Figure 2

shows that every one of the pinnacles relate to confront focused cubic structure of Ag-metal indicating that the examples arranged were of unadulterated silver metal nanoparticles. The determined molecule size and cross section parameter were accounted for in Table 1.

Table 1: Particle size and lattice parameter of silver nanoparticles.

Samples	Cappants (ml)	Angle (degree)	FWHM (β , degree)	Particle size (D) (nm)	Lattice parameter (nm)
Ag-1	OA (5ml)	38.162	0.19372	51	0.4081
Ag-2	OA (5ml)	38.162	0.17597	47	0.4080
Ag-3	OA (5ml)	38.149	0.17469	44	0.4082
Ag-4	TOP(5ml)	38.35	0.1798	51	0.4098
Ag-5	TOP(10ml)	38.29	0.2389	37	0.4061
Ag-6	TOP(20ml)	38.25	0.2561	31	0.4058
Ag-7	EG(100ml)	38.29	0.1851	40.5	0.4079
Ag-8	EG(100ml)	38.26	0.2351	36.7	0.4062
Ag-9	EG(100ml)	38.25	0.2042	37.8	0.4059

Figure 4 and 5 show the variation of thermopower (S) of silver nanoparticles with totally different particle sizes and cappants. For a comparison, the data for bulk atomic number 47 (Ag-bulk) is additionally enclosed from literature [Mcdonald 1962, Barnard1972]. it's clear that within the bulk atomic number 47, the sign of S is positive throughout the temperature vary (10-300K), indicating the holes as majority charge carriers as consequence of contribution from the necks of the Fermi surfaces [Mcdonald 1962]. In stark distinction, the S of the nanocrystalline silver show nearly mirrorreflection of that of bulk atomic number 47. Such associate observation indicates that the transport behavior within the samples is totally changed as compared to it of the majority. In

the vary ~85 K to 205 K, S exhibit positive values, indicating that the holes are majority charge carriers. On the opposite hand, S shows negative values within the temperature vary ~10 to eighty five K and 205 to three hundred K, indicating that the electrons are the majority charge carriers. Such behavior indicates that the general contributions of the bulk charge carriers are extremely temperature-dependent. These results clearly indicate dominant role of disorder a grain boundaries, which influence scattering of phonons and electrons in a significant way.

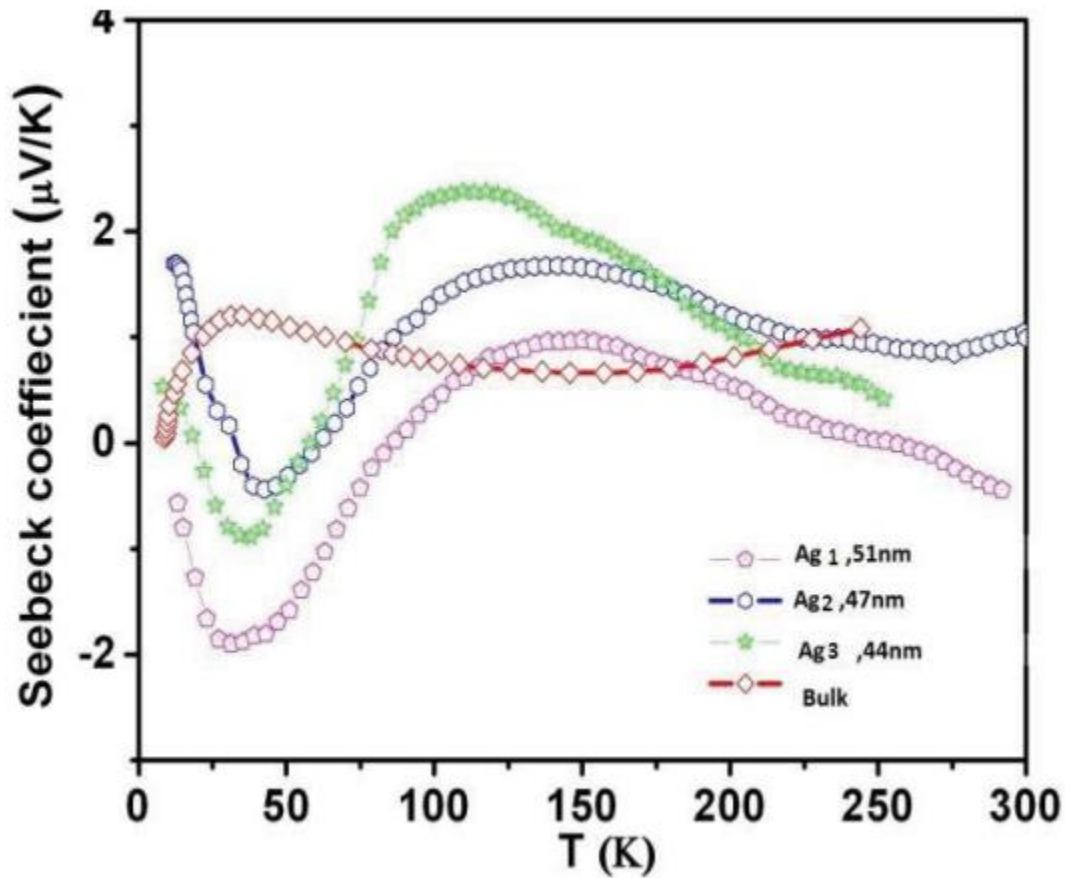


Figure 4. Variation of thermopower with temperature for Ag1, Ag2 and bulk samples.

Size effect on contributions from electrons and phonons is, in particular, attributed to their effective mean free path being reduced when D is comparable to or smaller than mean free path. In such situation, flow of phonon is restricted i.e. localized continually and transport of phonons is limited thereby decreasing phonon thermo power as D decreases.

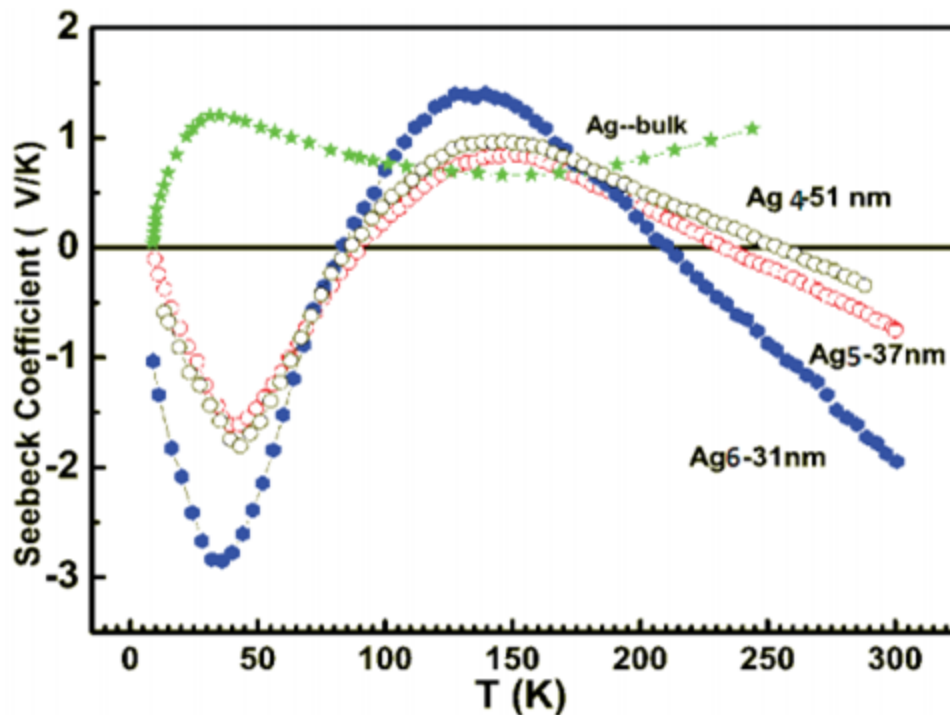


Figure 5. Variation of thermopower with temperature for Ag-4,Ag-5,Ag-6 and Bulk samples.

The dependence of optical properties on form was explored experimentally by playing UV-Visible absorption measurements of conductor NPs. The UV-Visible spectra of samples Ag-7, Ag-8 and Ag-9 are shown in Figure six.6. In metal nano particles, like in silver, the conductivity band and valence band lie terribly getting ready to one another within which electrons move freely. These free electrons give rise to a surface plasmon resonance (SPR) optical phenomenon occurring thanks to the collective oscillation of electrons of silver nano particles in resonance with the light wave. This absorption powerfully depends on the particle size (in the surface plasmon absorption bands the Doppler effect takes place with increase in particle size [McLellan et al. 2006, Mock et al. 2002]). The normalized absorption spectra of conductor NPs are shown within the Figure six.6. Surface plasmon optical phenomenon was discovered at 319 nm for all the 3 conductor NPs samples. The inset to the Figure six.6 indicates that the current samples don't show red-shift, presumably, thanks to same particle size for all the samples. It's instructive to say that the red-shift is discovered in earlier reports with increasing particle size of conductor NPs [Nie & Emory 1997, Anker 1202008]. specially, Wiley et al. have reported synthesis and optical properties of

silver nanobars and nanorice [Wiley et al. 2007]. Silver nanobars with rectangular side aspects and a mean ratio of two.7 are synthesized by modifying the concentration of bromide further to a polyol synthesis. The nanorice shape is achieved by subsequent misestimation of nanobars. thanks to their anisotropy, nanobars and nanorice peaks, scattering light-weight each within the visible and in the near-IR regions. The authors have explored the result of nano structure facet ratio and corner sharpness on the frequency of plasmon resonance. what is more, Mock et al. have conjointly found similar results [Mock et al. 2002]. it's attention-grabbing to point out that our samples don't show options in near-IR region. it's potential that our samples have similar size and form. Transmission microscopy (TEM) could any shade light-weight on the form on our samples.

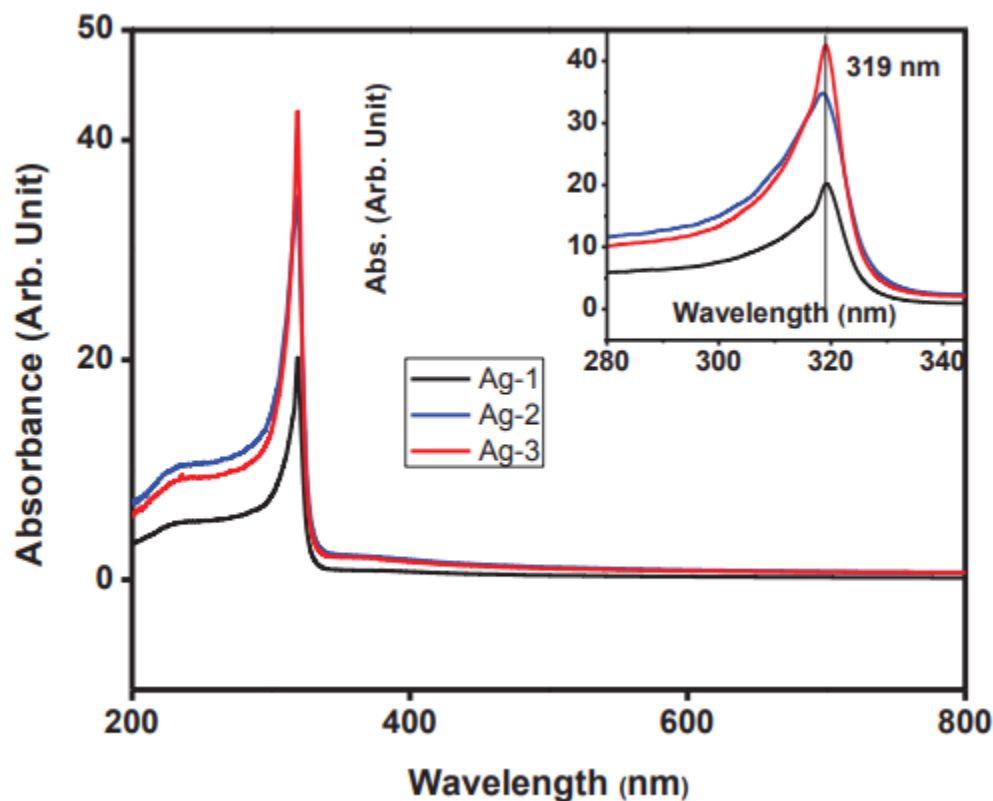


Figure 6. UV/Visible absorption spectra of Ag nano particle

Conclusions

Nanocrystalline silver nanoparticles were synthesized by thermal decomposition technique. The calculable particle size is found to be within the vary of 31-51 nm from XRD knowledge. As we tend to increase the number of capping in sample the

particle size was found to be decreasing. The magnitude of thermo power decreases because the particle size decreases. These results clearly indicate dominant role of disorder at grain boundaries that influence scattering of phonons and electrons in a very important approach. Noble metal NPs of average particle size of thirty eight nm are prepared through thermal reduction of silver acetate by EG. It's found that the particle size doesn't amend a lot of by variation of silver acetate concentration. UV/Vis spectrum analysis reveals the SPR optical phenomenon at 319 nm for all the 3 Ag NPs samples. We tend to believe that the red-shift in SPR can be discovered by victimization different Surfactant/Cappants.

References

1. [Abel et al. 2008] K. A. Abel, J. Shan, J. C. Boyer, F. Harris and Frank C. J. M. van Veggel, Chem. Mater. 20, 3794 (2008).
2. [Anker 2008] J. N. Anker, W. P. Hall, O. Lyandres, N. C. Shah, J. Zhao and R. P. Van Duyne, Nat. Mater. 7, 442 (2008).
3. [Anspoks & Kuzmin 2011] A. Anspoks, A. Kuzmin, J. Non-Cryst. Solids 357, 2604(2011).
4. [Barbaggiovanni et al. 2014] E. G. Barbaggiovanni, D. J. Lockwood, P. J. Simpson, L. V. Goncharova, Appl. Phys. Rev. 1, 011302 (2014).
5. [Basu et al. 2014] S. Basu, C. Nayak, A. K. Yadav, A. Agrawal, A. K. Poswal, D.
6. [Bhushan 2004] B. Bhushan, Handbook of Nanotechnology, Springer, Berlin (2004).
7. [Bishop et al. 2009] K. J. M. Bishop, C. F. Wimer, S. Soh and B. A. Grzybowski, Small 5, 1600 (2009).
8. [Bunker 2010] G. Bunker, Introduction to XAFS: a practical guide to X-ray absorption fine structure spectroscopy; Cambridge University Press: Cambridge, p 260 (2010).
9. [Carenco et al. 2010] S. Carenco, C. Ere, L. Nicole, C. Sanchez, P. Le Floch, and N. Mezaillies, Chem. Mater., 22, 1340 (2010).
10. [Chen et al. 2007] Y. Chen, D.L. Peng, D. Lin and X. Luo, Nanotech. 18, 505703 (2007).
11. [Chen et al. 2009] S. Chen, X. Zhang, Q. Zhang and W. Tan, Nanoscale Res. Lett.4, 1159 (2009).

12. [Christopher & Linic 2008] P. Christopher and S. Linic, J. Am. Chem. Soc. 13011264 (2008).
13. [Daniel & Astruc 2004] M. C. Daniel and D. Astruc, Chem. Rev. 104, 293 (2004).
14. [Das et al. 2011] S. Das, R. Rawat, N. P. Lalla and G. S. Okram, AIP Conf. Proc.1447, 851 (2011).
15. [Farn 2006] Richard J. Farn, Chemistry and Technology of Surfactants, BlackwellPublishing Ltd., 300 (2006).
16. [Gajbhiye et al. 2008] N. S. Gajbhiye, S. Sharma, A. K. Nigam and R. S. Ningthoujam, Chem. Phys. Lett., 466, 181 (2008).
17. [Hart et al. 2013] J. N. Hart, P. W. Maya, N. L. Allana, K. R. Hallamb, F. Claeysens, G. M. Fugea, M. Rudaa and P. J. Heard, J. Solid State Chem.,198, 466 (2013).
18. [Jeon et al. 2006] Y. T. Jeon, J. Y. Moon, G. H. Lee, J. Park and Y. Chang, J. Phys. Chem. B, 110, 1187 (2006).
19. [Jia et al. 2007] X. Jia, Y. Li, Q. Cheng, S. Zhang and B. Zhang, Europ. Polym. J. 43, 1123 (2007).
20. [Kelly et al. 2008] S. D. Kelly, D. Hesterberg and B. Ravel, Methods of Soil Analysis. Part 5. Mineralogical Methods, (Soil Science Society of America, Madison, USA), Chapter 14), (2008).